



## Room Temperature Ozone Detection using ZnO based Film Bulk Acoustic Resonator (FBAR)

Z. Wang,<sup>a,b,c</sup> X. Qiu,<sup>d,z</sup> J. Shi,<sup>a,c</sup> and H. Yu<sup>b,d</sup>

<sup>a</sup>School of Physics and <sup>c</sup>Key Laboratory of Acoustic and Photonic Materials and Devices of Ministry of Education, Wuhan University, Wuhan 430072, China

<sup>b</sup>School of Earth and Space Exploration and <sup>d</sup>School of Electrical, Computer and Energy Engineering, Arizona State University, Tempe, Arizona 85287, USA

This study describes room temperature ozone sensing with a ZnO based film bulk acoustic resonator (FBAR). The resonant frequency of FBAR decreased upon ozone exposure. For 1400 ppb ozone, the frequency downshift was 131 kHz with a response time of 12 s. The frequency decrease of the FBAR sensor was proposed to be due to the density increase of the ZnO film. Ozone can be adsorbed on the ZnO surface by capturing free electrons from the film, which increases the film density. An analytical model was developed to predict the relationship between resonant frequency and ozone concentration. In agreement with the experiment, a hyperbolic function was obtained.

© 2011 The Electrochemical Society. [DOI: 10.1149/2.054201jes] All rights reserved.

Manuscript submitted August 15, 2011; revised manuscript received September 20, 2011. Published December 14, 2011.

Ozone is the Earth's protective layer against UV radiation in the atmosphere. At the ground level, however, ozone is one of the harmful pollutants and greenhouse gases, and closely linked to human activities including a variety of industrial processes ranging from food storage to pharmaceutical, textile, and chemical processing. Air quality standards established by the U.S. Environmental Protection Agency (EPA) in 2008 state that ozone concentration levels must be kept below 75 ppb. UV adsorption is the most common detection method for ozone.<sup>1</sup> Though this method is reliable and highly sensitive, there are drawbacks: the cost is high, the detector is large, and the entire apparatus is complex. Metal oxide based ozone sensors offer an alternative mechanism. This electrochemical detection method uses ZnO,<sup>2</sup> WO<sub>3</sub>,<sup>3</sup> and In<sub>2</sub>O<sub>3</sub><sup>4</sup> as sensing materials and has the advantages of compact size, low cost, and high sensitivity. However, most of these detectors must operate at high temperatures (usually over 200°C), and in some cases, they also require UV illumination to enhance sensing performance at room temperature.

In this study, we report the investigation of a room temperature ozone sensing device that employs a ZnO based film bulk acoustic resonator (FBAR). FBAR usually consists of a sputtered piezoelectric thin film (ZnO) sandwiched between two metal layers (top and bottom electrodes). A resonance condition occurs if the thickness of piezoelectric thin film is equal to an integer multiple of a half of the acoustic wavelength. In recent years, FBAR has been developed to be a filter<sup>5</sup> as well as a high sensitivity mass, ultraviolet and humidity sensor.<sup>6-9</sup> The FBAR ozone sensor's design and characterization are described and the mechanism for the frequency downshift of the FBAR in the presence of ozone is discussed.

### Experimental

The schematic structure of the FBAR ozone sensor is shown in Figure 1. The device was fabricated on top of a SiN (0.6 μm) diaphragm. A sputtered ZnO film (1.2 μm) was used both as the ozone sensitive layer and the piezoelectric actuation layer for the FBAR sensor. The top and bottom electrodes were made of Cr/Au (0.02/0.2 μm) and Al (0.2 μm), respectively. Due to the surface roughness of the film, the top Cr/Au electrode did not form a conformal coating on the ZnO. Thus, there are some small gaps between ZnO and the electrode at certain locations, and these gaps can provide a channel for ozone to reach the ZnO layer.

The fabrication process of the FBAR was as follows. First, a SiN layer was deposited on a Si wafer (100) with low-pressure chemical

vapor deposition (LPCVD). Then the Si wafer was etched from the backside anisotropically in potassium hydroxide (KOH) to form the cavity. Next, the bottom Al electrode was deposited by electron-beam (e-beam) evaporation and patterned on top of the SiN film using wet chemical etching. ZnO was radio-frequency (RF) sputtered and etched to form the desired pattern. The last step was the e-beam deposition and patterning of top Cr/Au electrode by lift-off.

The ZnO film was characterized by X-ray diffraction (XRD) (Fig. 1). Only the Bragg reflection corresponding to (002) planes was observed, indicating that the film had a preferred growth orientation along the wurtzite C axis, which was normal to the silicon substrate. The entire sensor was encapsulated in a chamber to control the ozone concentration. A UV ozone generator (UVP Corp) was employed to provide ozone, and a commercial ozone monitor (2B Technologies Inc) was applied to calibrate the ozone concentration. Pure oxygen was used to purge the chamber after ozone measurement. The FBAR was tested on a probe station with Ground-Signal-Ground 150 micron pitch probes (Cascade Microtech Inc). The calibration was carried out with an impedance standard substrate using a short-open-load (SOL) method. The resonant frequency of the FBAR was monitored with an Agilent E5071C network analyzer (Agilent) and recorded by a LabVIEW program (National Instruments).

### Results and Discussion

The measured resonant frequency of the FBAR was 1.38 GHz. Figure 2a shows the response of the FBAR sensor to 1400 ppb ozone at room temperature. A frequency downshift of 131 kHz was observed with a response time of 12 s. Three testing cycles were recorded to demonstrate the repeatability and stability of the sensor. The increase of temperature may result in a frequency downshift due to the negative temperature coefficient of resonant frequency (TCF) of ZnO based FBAR.<sup>10</sup> The measured TCF for the ozone sensor was -72.7 ppm/°C. The sensor temperature was monitored during ozone testing, and a change of less than 0.1°C was observed. Therefore, the frequency downshift cannot be explained by the TCF of the device and was in fact the result of interaction between ozone and the ZnO film on the FBAR.

The resonant frequency of the FBAR can be determined from the following two equations:

$$v = \sqrt{\frac{E}{\rho}} \quad [1]$$

$$f = \frac{v}{2d} \quad [2]$$

<sup>z</sup> E-mail: xqiu5@asu.edu

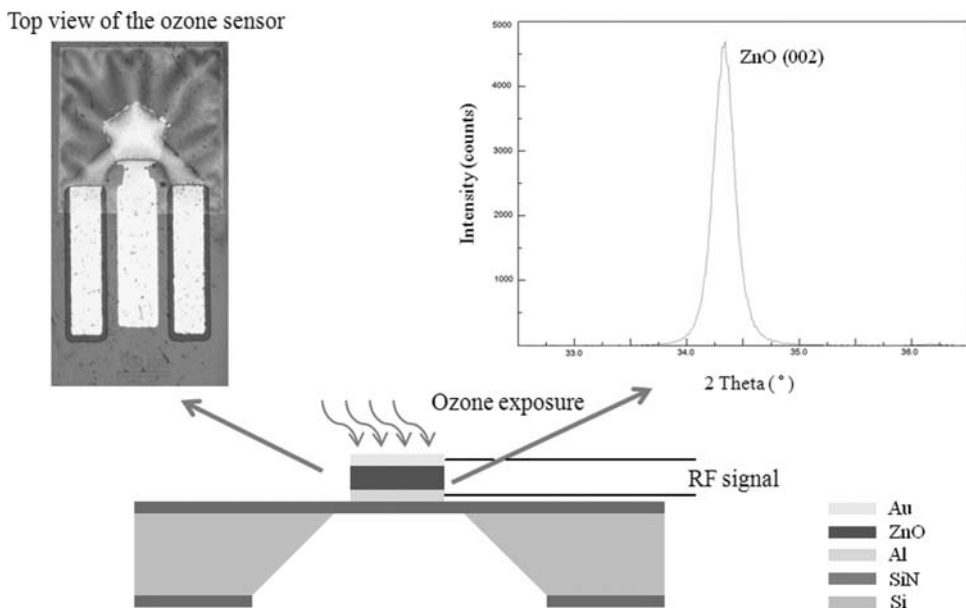


**Figure 1.** Schematic cross-sectional structure of the FBAR ozone sensor with a photograph of the top view of a fabricated device on the left and an XRD trace of the ZnO film illustrating that it has (002) crystal orientation on the right.

where  $E$ ,  $\rho$  and  $d$  are, respectively, the elastic constant, density and thickness of the ZnO film. In the equation,  $v$  is the acoustic velocity inside the film and  $f$  is the resonant frequency of the FBAR. Thus, a frequency downshift is likely due to the density increase of the ZnO film upon ozone exposure. Ozone can capture free electrons from the ZnO film and it will be adsorbed on the ZnO surface (both film surface and grain boundary surface) as negative oxygen ions, resulting in an increase in film density. Because of the increased density, the acoustic velocity decreases, as does the resonant frequency of the FBAR. During the oxygen purge stage, oxygen ions generated by ozone will be desorbed due to the decreased ozone concentration.

During the process, the density of the ZnO film decreases, resulting in an increase of resonant frequency. Figure 2b illustrates the sensing mechanism of the FBAR ozone sensor.

The electric resistance of a semiconductor gas sensor exposed to a target gas (partial pressure  $P$ ) is known to be proportional to  $P^n$ , where  $n$  is a constant fairly specific to the kind of target gas (power law). Yamazoe et al. established a theoretical basis to the power law combining a depletion theory of semiconductor with the dynamics of adsorption and/or reactions of gases on the surface.<sup>11</sup> By extending their work to address density change in a semiconductor gas sensor, a theoretical model for the ozone response of the ZnO based FBAR was

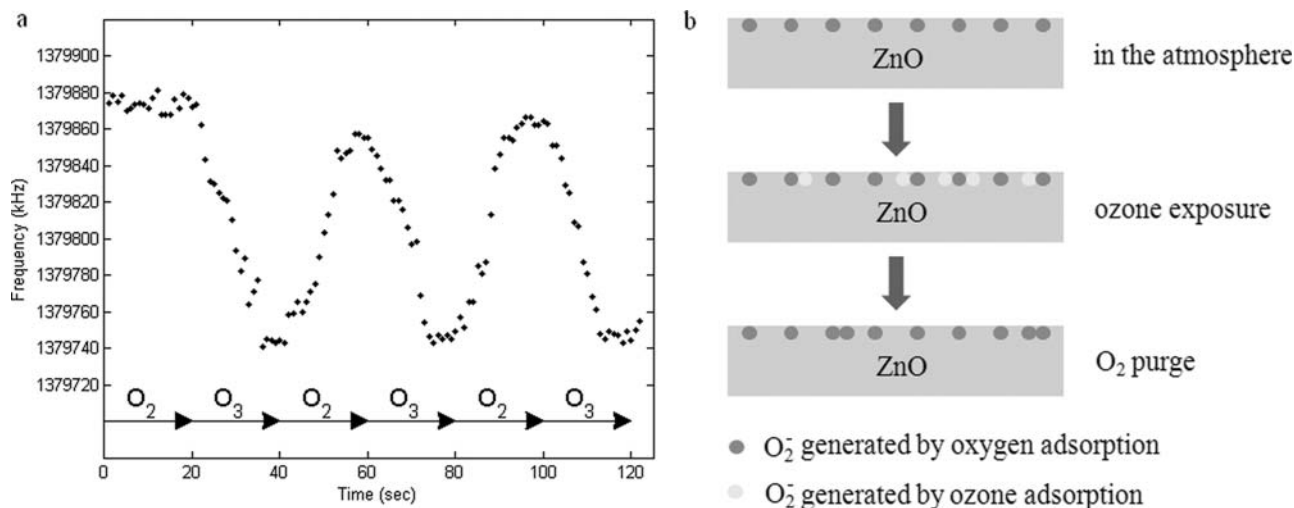


**Figure 2.** (a) The response of the FBAR sensor to 1400 ppb ozone at room temperature. A frequency downshift of 131 kHz was observed with a response time of 12 s. Three testing cycles were recorded to demonstrate the repeatability and stability of the sensor; (b) The sensing mechanism of the FBAR ozone sensor. Ozone can capture free electrons from the ZnO film. It will be adsorbed on the ZnO surface as negative oxygen ions, resulting in an increase in film density. Because of the increased density, the acoustic velocity decreases, as does the resonant frequency of the FBAR. During the oxygen purge stage, oxygen ions generated by ozone will be desorbed due to the decreased ozone concentration. During the process, the density of the ZnO film decreases, resulting in an increase of resonant frequency. Due to the high oxygen concentration during oxygen purge compared to the atmospheric case, additional oxygen is adsorbed on the ZnO film, which prevents the resonant frequency recovering to the original value, as shown in (a).

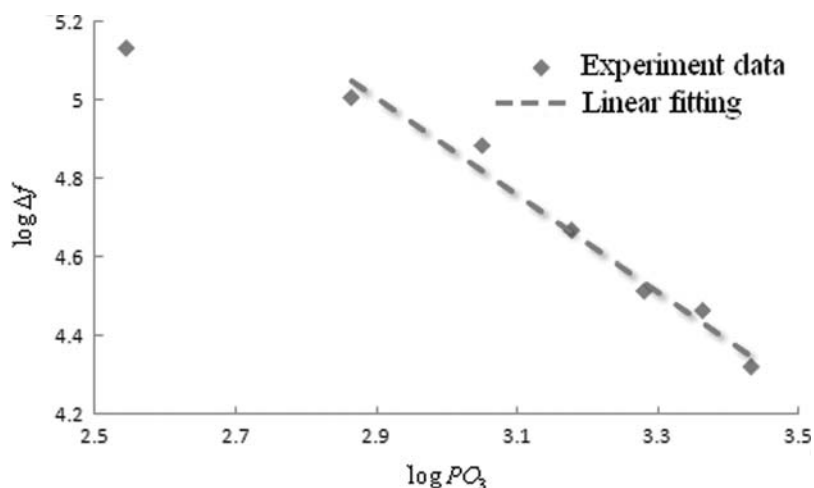


**Figure 3.** The shift of resonant frequency with ozone concentration. At low concentration end, ozone adsorption is no longer the dominant process. Therefore, the data deviates from the linear fitting in this region.

developed. According to Yamazoe et al., the density of conduction electrons at surface  $[e]$  can be expressed as:

$$[e] = N_d \exp\left(-\frac{m^2}{2}\right) \quad [3]$$

where  $N_d$  is the density of donors and  $m$  is the reduced depletion depth. The amount of oxygen adsorption/desorption at each grain-boundary is proportional to  $[e]$ . The relative density change,  $\Delta\rho$ , induced by adsorption/desorption of oxygen is therefore proportional to  $[e]$ .

The frequency shift  $\Delta f$  induced by density change can be formulated as follows.<sup>9</sup>

$$\Delta f \approx \frac{\sqrt{E}}{2d} \cdot \frac{\left(1 - 1 - \frac{1}{2} \frac{\Delta\rho}{\rho}\right)}{\sqrt{\rho}} = -\frac{\sqrt{E}}{4d\rho\sqrt{\rho}} \Delta\rho \quad [4]$$

The frequency shift  $\Delta f$  is therefore proportional to  $\Delta\rho$  and thus, also proportional to  $[e]$ .

At room temperature, both oxygen and ozone can be adsorbed on the surface of ZnO by capturing free electrons from the film.<sup>12</sup>



The rate of accumulation of  $O_2^-$  is zero at equilibrium, so,

$$k_{o1} P O_2 [e] + k_{o2} P O_3 [e] = [O_2^-] \quad [7]$$

where  $k_{o1}$  and  $k_{o2}$  are the equilibrium constants of oxygen and ozone adsorption, respectively. The brackets mean the density of  $O_2^-$  per unit area or that of electrons per unit volume,  $P O_2$  is the partial pressure of oxygen, and  $P O_3$  is the partial pressure of ozone.<sup>9</sup>

Assuming there are no electron-trapping sites other than  $O_2^-$  on the surface, the  $O_2^-$  ions would be solely responsible for the surface charge density:

$$[O_2^-] = N_d \omega \quad [8]$$

Here  $\omega$  is the depletion depth, and  $\omega = m L_D$ , where  $L_D$  is the Debye length.<sup>11</sup>

Inserting equation 3 and 8 into 7 yields the following:

$$k_{o1} P O_2 \exp\left(-\frac{m^2}{2}\right) + k_{o2} P O_3 \exp\left(-\frac{m^2}{2}\right) = \omega \quad [9]$$

Reaction 6 is the dominant process during ozone sensing, thus

$$k_{o2} P O_3 \gg k_{o1} P O_2 \quad [10]$$

Therefore, the calculated power law exponent  $n$ , defined as  $d(\log \Delta f)/d(\log P O_3)$  is

$$\frac{d(\log \Delta f)}{d(\log P O_3)} = -1 + \frac{1}{1 + m^2} \quad [11]$$

where  $m$  is sufficiently large under usual conditions.<sup>11</sup> Thus  $n$  is around  $-1$ , which means the relationship between resonant frequency and ozone concentration is hyperbolic, which is in agreement with the experiment results (Fig. 3). All the data were measured at room temperature. One point needs to be noticed here is that at low concentration end, ozone adsorption is no longer the dominant process. Equation 10 is not valid. Therefore, the data deviates from the linear fitting in this region (Fig. 3).

As discussed above, ozone competes with oxygen for adsorption onto the ZnO surface. To achieve ozone sensing, either a high ozone concentration ( $P O_3$ ) or large ozone adsorption coefficient ( $k_{o2}$ ) is required. High temperature or UV can be used to enhance the ozone adsorption, which is why many metal oxide ozone sensors operate under such conditions.

## Conclusions

In conclusion, a room temperature ozone sensor was developed using ZnO based film bulk acoustic resonator. A frequency down-shift was observed upon ozone exposure. The sensor output was a frequency change-suitable for integration with a wireless sensor network. The working principle of the FBAR ozone sensor was attributed to the density increase of ZnO caused by ozone adsorption. Moreover, both the experiment results and the theoretical analysis showed the relationship between resonant frequency and ozone concentration to be hyperbolic. The success of this FBAR sensor demonstrates potentials for detecting other oxidizing gases in future studies.

## Acknowledgments

This research was partially funded by NASA Astrobiology Institute (follow the elements) and ASU dissertation fellowship (Xiaotun Qiu) and the Chinese Scholarship Council (Ziyu Wang). Authors Z. Wang and X. Qiu both contributed equally in this work.

## References

1. D. Daumont, J. Brion, J. Charbonnier, and J. Malicet, *J. Atmospheric Chem.*, **15**, 145 (1992).
2. R. Martinez, E. Fortunato, P. Nunes, I. Ferreira, A. Marques, M. Bender, N. Katsarakis, V. Cimalla, and G. Kiriakidis, *J. Appl. Phys.*, **96**, 1398 (2004).

3. K. Aguir, C. Lemire, and D. B. B. Lollman, *Sens. Actuators B.*, **84**, 1 (2002).
4. E. Gagaoudakis, M. Bender, and E. Douloufakis, *Sens. Actuators B.*, **80**, 155 (2001).
5. M. Ueda, M. Hara, S. Taniguchi, T. Yokoyama, T. Nishihara, K. Hashimoto, and Y. Satoh, *Jpn. J. Appl. Phys.*, **47**, 4007 (2008).
6. H. Zhang and E. S. Kim, *J. Microelectromech. Syst.*, **14**, 699 (2005).
7. X. Qiu, J. Zhu, J. Oiler, C. Yu, Z. Wang, and H. Yu, *Appl. Phys. Lett.*, **94**, 151917 (2009).
8. X. Qiu, J. Oiler, J. Zhu, Z. Wang, R. Tang, C. Yu, and H. Yu, *Electrochemical and Solid-State Letters.*, **13**, J65 (2010).
9. X. Qiu, R. Tang, J. Zhu, J. Oiler, C. Yu, Z. Wang, and H. Yu, *Sens. Actuators B.*, **147**, 381 (2010).
10. X. Qiu, Z. Wang, J. Zhu, J. Oiler, R. Tang, C. Yu, and H. Yu, *IEEE Trans. Ultrason. Ferroelect. Freq. Contr.*, **57**, 1902 (2010).
11. N. Yamazoe and K. Shimanoe, *Sens. Actuators B.*, **128**, 566 (2008).
12. M. Takata, D. Tsubone, and H. Yanagida, *J. Am. Ceram. Soc.*, **59**, 4 (1976).